

DOI: <http://doi.org/10.52716/jprs.v14i2.867>

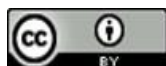
## Biosynthesis of Fe/Pd Bimetallic Nanoparticles and Used for Removal of Synthetic Oily Wastewater

Ahmed K. Hassan\*, Luay Q. Hashim, Ahmed M. Rezoqi, Mohammed F. Hashim

Environment, Water and Renewable Energy Directorate, Ministry of Science and Technology, Baghdad, Iraq.

\*Corresponding Author E-mail: [ahmedkhh71@gmail.com](mailto:ahmedkhh71@gmail.com)

Received 24/12/2023, Revised 21/02/2024, Accepted 25/02/2024, Published 12/06/2024

This work is licensed under a [Creative Commons Attribution 4.0 International License](https://creativecommons.org/licenses/by/4.0/).

### Abstract

Eucalyptus plant leaves aqueous extract was used to produce a green bimetallic Fe/Pd nanoparticles (G-Fe/Pd NPs) catalyst for the degradation of synthetic oily effluent. Using Brunauer-Emmett-Teller (BET) analysis, Fourier-transform infrared spectroscopy (FTIR), particle size, and a zeta potential analyzer, the synthesized G Fe/Pd NPs were evaluated. G-Fe/Pd NPs have been found to contain nanoparticles, with a mean size of 182 nm and a surface area of 5.106 m<sup>2</sup>/g. The resulting nanoparticles were then used as a catalyst for a Fenton-like reaction. The amount of green catalyst G-Fe/Pd NPs (0.125-0.5 g/L), H<sub>2</sub>O<sub>2</sub> concentration (15-37.5 mmol/L), pH (3-7), and temperature (25-45°C) all have a significant impact on the degradation efficiency of synthetic oily wastewater. Batch experiments showed that 88.9% degraded chemical oxygen demand (COD) from synthetic oily wastewater within the optimum conditions of peroxide concentration, catalyst dose, pH, and temperature which were 30.0 mmol/L, 0.375 g/L, 3, and 45°C respectively along with 60 min contact time. The results of kinetic models showed that oily wastewater removal followed the Behnajady-Modirshahla-Ghanbary (BMG) model. Finally, the thermodynamic study of the reaction was also examined and concluded to endothermic reaction with an enthalpy of 37.39 kJ/mol.

**Keywords:** Biosynthesis, Fe/Pd bimetals, Fenton-like, Oily wastewater removal, Kinetic model, and Thermodynamic function.

التخليق الحيوي لجسيمات Fe/Pd النانوية ثنائية الفلز واستخدامها لإزالة المياه الملوثة بالمشتقات النفطية المصنعة

### الخلاصة:

تم استخدام المستخلص المائي لأوراق نبات شجرة اليوكالبتوس لإنتاج محفز أخضر لجسيمات الحديد/بلاديوم ثنائية الفلز النانوية (G-Fe/Pd NPs) لإزالة الملوثات السائلة بالمشتقات النفطية المصنعة. تم تشخيص المركب المحضر G-Fe/Pd NPs عن طريق استخدام تحليل Brunauer-Emmett-Teller (BET)، والتحليل الطيفي للأشعة تحت الحمراء لتحويل فورييه (FTIR)، وقياس حجم الجسيمات، وقياس جهد زيتا. أظهرت نتائج التشخيص بأن جسيمات G-Fe/Pd NPs لها معدل اقطار حوالي 182 نانومتر بينما كانت مساحتها السطحية 5.106 م<sup>2</sup>/غم. فيما بعد استخدمت الجسيمات النانوية الناتجة

كعامل مساعد في تفاعلات الشبيهة بالفنتون. حيث أن كفاءة تحلل المياه الملوثة بالمشتقات النفطية اعتمدت بشكل كبير على تركيز كمية المحفز الأخضر (0.125-0.5 G-Fe/Pd NPs /جم/لتر)، وتركيز ( $H_2O_2$  15-37.5 ملليمول/لتر)، ودرجة الحموضة (3-7)، ودرجة الحرارة (25-45 درجة مئوية). أظهرت التجارب أن نسبة كفاءة الإزالة 88.9% للمياه الملوثة بالمشتقات النفطية من حيث المتطلب الكيميائي للاوكسجين (COD) وعند الظروف المثلى من تركيز البيروكسيد، والكمية للعامل المساعد، ودرجة الحموضة، ودرجة الحرارة، كانت 30.0 ملليمول/ لتر، 0.375 جم/ لتر، 3، و 45 درجة مئوية على التوالي وبعد مرور 60 دقيقة من وقت التفاعل. كما أظهرت نتائج النماذج الحركية أن إزالة المياه الملوثة بالمشتقات النفطية تتبع نموذج حركي من الموديل BMG. أخيراً، تم دراسة الديناميكية الحرارية للتفاعل وخلصت إلى ان التفاعل ماصاً للحرارة وله انتالبي مقدارها 37.39 كيلوجول/مول.

## 1. Introduction:

The industrial sector is a significant contributor to water pollution, as it produces and discharges various types of toxic compounds into water effluents [1]. Organic pollutants, including petroleum hydrocarbons, pose a significant threat to the environment and human health when released into aquatic systems [2]. Unfortunately, petroleum hydrocarbons are persistent organic contaminants that can have detrimental effects on the environment and can have various negative effects on both humans and the aquatic ecosystem [3-4]. To mitigate the negative impacts of petroleum hydrocarbon pollutants, stricter regulations, and wastewater treatment processes are needed to ensure the effective removal and reduction of these contaminants before they are discharged into the environment [5]. Currently, several modern techniques of treating oily wastewater are being consistently used [6-7]. The selection of the appropriate technique depends on factors like the level of contamination, environmental conditions, and the desired remediation goals. Advanced oxidation processes (AOPs) have received considerable attention as a potential strategy compared to conventional methods because of how well they degrade and mineralize contaminants in wastewater [8]. Heterogeneous Fenton-like oxidation, which relies on the interaction between solid iron (as a catalyst) and hydrogen peroxide (as an oxidant), produces hydroxyl free radicals ( $\bullet OH$ ), a highly reactive species [9-10].

In general, green nanotechnology involves the use of biological sources, such as bacteria, fungi, or plants, in the production of nanomaterials using a variety of biotechnological methods [11]. The resulting nanoparticles are environmentally safe and devoid of hazardous substances. The capping and reducing agents such as flavonoids, polyphenols, and other reducing compounds found in plant extract can convert the metal ion to zero-valent and prevent them from aggregating [12]. These plant extracts offer several benefits, including the fact that they are inexpensive, non-toxic, and free of compounds with negative side effects. By using a second

catalyst like Cu, Pt, Pd, or Ni, bimetal is utilized to shield nanoparticles from oxidizing to stop this process [13-14].

The purpose of this work is to investigate the removal of synthetic oily wastewater by a Fenton-like process employing an inexpensive and environmentally safe catalyst. First, green synthesis of bimetallic iron/palladium nanoparticles (G-Fe/Pd NPs) was achieved by reducing the iron and palladium salts with an extract from eucalyptus plant leaves. Second, study different experimental parameters that affect for removal of oily wastewater using a batch Fenton-like oxidation. The effects of pH, temperature, G-Fe/Pd-NPs dose, and H<sub>2</sub>O<sub>2</sub> concentration were all investigated in each step. Thirdly, study the kinetics and thermodynamics of Fenton-like reactions to ascertain the processes' type and rate of operation.

## 2. Material and Methods

In this study, all substances were of the analytical grade, and all experimental components used distilled water. The Ministry of Science and Technology's park was used to harvest the Eucalyptus leaves, which were then dried at 50°C in an electric oven. While palladium chloride (PdCl<sub>2</sub>) (Pd 59–60%) was obtained from CDH, India, anhydrous ferric chloride (FeCl<sub>3</sub>), hydrogen peroxide (30% weight per weight), and sodium sulfite (Na<sub>2</sub>SO<sub>3</sub>) were purchased from Sigma-Aldrich. The synthetic pollutant was commercial diesel oil from Iraq, and the emulsifier was sodium dodecyl sulfate (SDS) (C<sub>12</sub>H<sub>25</sub>Na<sub>4</sub>S). The pH was adjusted using sodium hydroxide (NaOH) and sulfuric acid (H<sub>2</sub>SO<sub>4</sub>), both of which were acquired from AppliChem (GmbH).

### 2.1. Preparation of the synthetic oily wastewater

Following the steps given in “References [15], and [16]”, we prepared the oily wastewater as follows:

The synthetic oily emulsion was prepared by gradually adding 15 mL of Iraqi diesel oil to 985 mL of distilled water while stirring the mixture at 300 rpm, along with 0.05 g of SDS emulsifier. After filtering the emulsion solution with Whatman 22-μm filter paper, an emulsion with a chemical oxygen demand (COD) concentration of 200±11 mgO<sub>2</sub>/L was obtained.

### 2.2. Synthesis of green iron/palladium nanoparticles G- Fe/Pd-NPs

The method used for synthesizing the G- Fe/Pd-NPs was somewhat modified from that disclosed in the earlier work “References [13], and [17]”. The steps were as follows: In an

electric oven set to 50°C, humid Eucalyptus leaves were gathered and dried. To make the bioactive extract, 10.0 g of dry, finely powdered eucalyptus leaves powder was dissolved in 250 mL of distilled water. A hotplate set to 85°C was used to heat the solution for 30 minutes. After that, the extract was cooled to room temperature and filtered through a 0.45- $\mu\text{m}$  membrane filter to remove the suspended eucalyptus particles. The following step was mixing 1.6 g of solid  $\text{FeCl}_3$  with 100 mL of distilled water to produce a solution that contained 0.10 mol/L of ferric chloride. Weighing 0.08 g of solid  $\text{PdCl}_2$  in 100 mL distilled water resulted in the preparation of another  $\text{PdCl}_2$  solution (4.5 mmol/L). These two solutions were thoroughly dissolved before; the contaminants were eliminated by filtering them using a 0.45- $\mu\text{m}$  membrane filter. The combination of solutions of ( $\text{FeCl}_3$  and  $\text{PdCl}_2$ ) was slowly added to the Eucalyptus extract solution for 30 min at room temperature while being continuously stirred at a magnetic stirring rate of 300 rpm. The color of the mixture shifted from yellow to black once the addition was finished. This proved that  $\text{Fe}^{3+}$  and  $\text{Pd}^{2+}$  had been converted into  $\text{Fe}^0$  and  $\text{Pd}^0$  nanoparticles, respectively. The solution was then brought to a pH of 6.0 and agitated continuously for 15 minutes. Following an hour of the solution standing, the black precipitate of Fe/Pd nanoparticles was removed using vacuum filtering and filter paper with a 0.45- $\mu\text{m}$  pore size. The G- Fe/Pd-NPs were dried in an oven at 50°C for the whole night before being milled into a fine powder.

### 2.3. Characterization of G-Fe/Pd NPs

To describe the functional groups of the G-Fe/Pd NPs, the Fourier transform infrared spectroscope (FTIR) was employed. Shimadzu spectrophotometer was used to conduct the FTIR analysis in the spectrum region of 4000 to 400  $\text{cm}^{-1}$ . To study the electrophoretic behavior of the fluid, the Zeta Potential Analyzer model (NanoBrook ZetaPlus) was utilized to assess the stability of produced G-Fe/Pd NPs. The zeta potential of any nanoparticles might be positive at low pH levels or negative at high pH values. Zeta potential measurements had a pH of around 6. Additionally, the particles' sizes ranged from 10 nm to 300 nm, depending on particle density can be measured by Zeta Plus.

### 2.4. Batch experiments for removal of oily wastewater

According to the following methodology, batch evaluations were carried out in this study to evaluate oily wastewater removal effectiveness. In the Fenton-like oxidation studies, the effect of G-Fe/Pd NPs amount was investigated in the concentration range of 0.125 to 0.5 g/L on the

oxidation of 1.0 L of a synthetic oily solution containing  $200 \pm 11$  mgO<sub>2</sub>/L of COD at a fixed concentration of 22.5 mmol/L hydrogen peroxide (H<sub>2</sub>O<sub>2</sub>) and pH of 3. Later, at a pH of 3, the ideal dosage of G-Fe/Pd NPs (0.375 g/L) and the influence of H<sub>2</sub>O<sub>2</sub> concentration (between 15 and 37.5 mmol/L) on the degradation of oily wastewater were assessed. Three different pH values (3, 5, and 7) were used in experiments to see which was the most effective for allowing oily wastewater to degrade. Additionally, the effects of the reaction temperature in the range of 25-45°C were investigated. The standard photometric method 5220D was used to calculate the chemical oxygen demand (COD). By comparing instrument response (Absorbance) against a reference concentration of potassium hydrogen phthalate, as illustrated in Figure (1), we established a calibration curve using the photometric method 5220D. Then the sample response with the standard curve was evaluated, to determine the sample concentration. While degradation efficiency percentage, DE (%) for oily wastewater was calculated according to Equation (1):

$$DE(\%) = \frac{COD_0 - COD_t}{COD_0} \times 100 \quad (1)$$

where COD<sub>0</sub> is the initial concentration of COD of the oily wastewater, and COD<sub>t</sub> is the concentration of COD at time t.

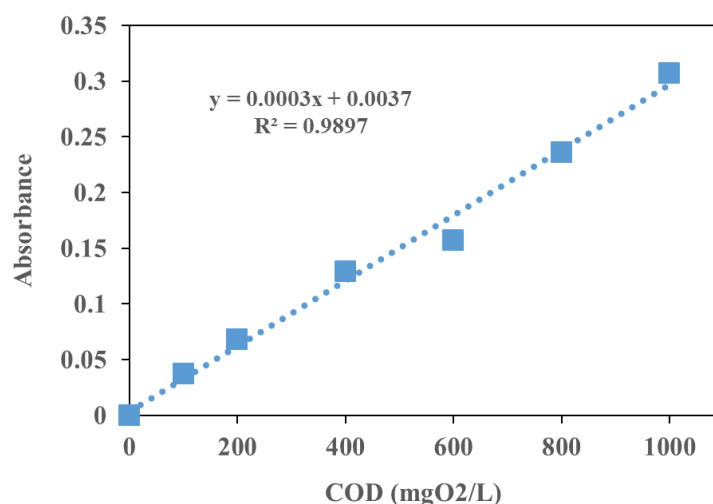


Fig. (1): Calibration curve for COD

### 3. Results and Discussion

#### 3.1 Characterization of the catalyst G-Fe/Pd NPs

The zeta potential analyzer was used to assess the green catalyst G-Fe/Pd nanoparticle size. This method made use of electrophoretic light scattering (ELS), The nanoparticle particles

had an average diameter of 182 nm. High zeta potential values provide nanoparticle stability to prevent aggregation, whereas low potential causes flocculation. The overall stability of G-Fe/Pd-NPs was demonstrated by a moderately negative value at (-31.0 mV) from zeta analysis, as shown in Figure (2). This stability results from the presence of phenolic chemicals in the eucalyptus plant leaf extract [18].

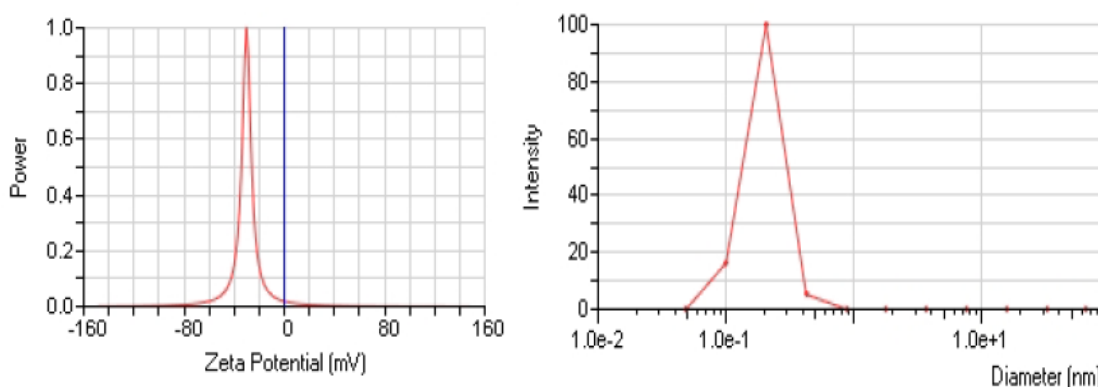


**Fig. (2): Zeta analysis (a) potential (b) particles size for G-Fe/Pd-NPs**

The findings of the G-Fe/Pd-NPs surface area obtained using the BET approach are displayed in Table (1). According to the categorization of the IUPAC, which defined the pore size as macropore (more than 50 nm), mesopore (2 to 50 nm), super micropore (0.7 to 2 nm), and ultra-micropore (less than 0.7 nm) [13], the pore size for G-Fe/Pd-NPs in this investigation was 50.4 nm, which may be classified as a mesopore. These diameters of holes therefore provide better stability by acting as a shielding agent to avoid the severe reaction conditions of the nanoparticles' active sites [18].

**Table (1) BET parameters for G-Fe/Pd-NPs**

Parameter	Value
BET (m <sup>2</sup> /g)	5.106
Pore size (nm)	50.4
Pore volume (cm <sup>3</sup> /g)	0.019

In order to ensure that the functional group of the green catalyst G-Fe/Pd-NPs is as shown in Figure (3), the FTIR is obtained in the band range 400-4000 cm<sup>-1</sup>. The polyphenol compounds that play a significant role in the reduction of the Fe/Pd metals and subsequent creation of bimetallic nanoparticles are responsible for the O-H stretching vibrations shown in the band 3392 cm<sup>-1</sup>. The presence of polyphenols in eucalyptus leaves is shown by the C=C group in the

produced nanoparticles, which can be seen at band  $1620\text{ cm}^{-1}$ . These substances contribute to the reduction of G-Fe/Pd NPs production. While bands at  $1190$  and  $1160\text{ cm}^{-1}$  belong to C-OH bending, respectively, bands at  $1433$  and  $1429\text{ cm}^{-1}$  were associated with the aromatic ring as seen in Figure (3) “in press” [19]. The (Fe-O) stretching relates to the bands found at  $750\text{ cm}^{-1}$ , and the vibration bandwidth between  $478\text{ cm}^{-1}$  might be attributed to Fe/Pd nanoparticles [20].

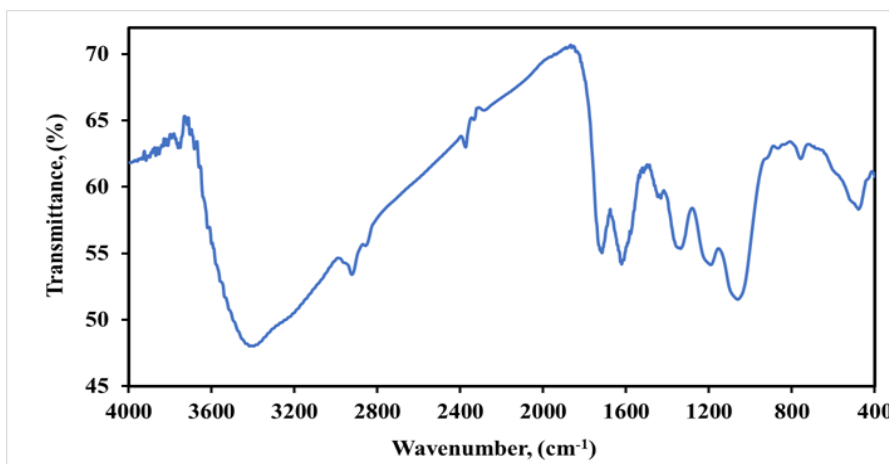
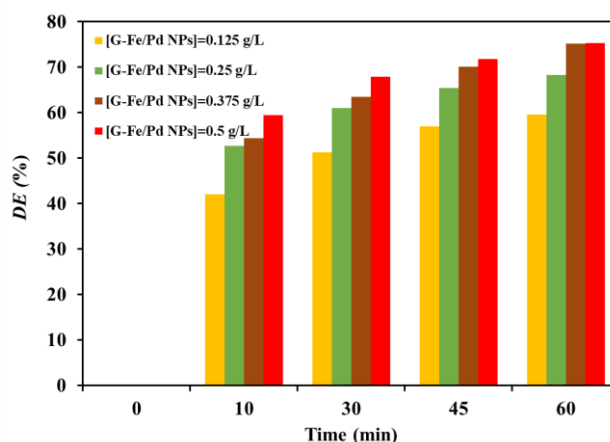


Fig. (3): FTIR spectra of G-Fe/Pd-NPs

### 3.2 Effect of the amount of G-Fe/Pd NPs

With doses ranging from 0.125 to 0.5 g/L, the impact of green catalyst G-Fe/Pd NPs loading on the removal of oily wastewater was investigated. The first stage is maintaining the  $\text{H}_2\text{O}_2$  concentration at 22.5 mmol/L and doing several experiments with varying concentrations of green catalyst to remove synthetic oily solution containing  $200 \pm 11\text{ mgO}_2/\text{L}$  of COD at original pH 3 and room temperature. According to Figure (4), after 60 minutes of the Fenton-like reaction, 75.1% of the oily wastewater was removed using 0.375 g/L of G-Fe/Pd NPs, but only 59.5% was accomplished using 0.125 g/L of G-Fe/Pd NPs. The increased accessibility of active sites throughout the whole surface area of the green catalyst G-Fe/Pd NPs may be responsible for this [12]. There is no significant enhancement in the degradation efficiency when the amount of the green catalyst is increased. Therefore, we chose 0.375 g/L as the optimum concentration.



**Fig. (4): Effect of G-Fe/Pd NPs dose**

### 3.3. Effect of H<sub>2</sub>O<sub>2</sub> concentration

The required amount of hydrogen peroxide (H<sub>2</sub>O<sub>2</sub>) is a crucial factor in achieving the highest level of oily degradation from aqueous solutions [15]. The first step is maintaining the green catalyst G-Fe/Pd NPs at its ideal concentration of 0.375 g/L and researching the effects of various H<sub>2</sub>O<sub>2</sub> concentrations on the removal of 200±11 mgO<sub>2</sub>/L of COD oily aqueous solution at starting pH 3.0 and room temperature. Figure (5) indicates evidence that the effectiveness of degradation increased as hydrogen peroxide concentration increased because more hydrogen peroxide results in a higher generation of the hydroxyl free radical (•OH). According to Figure (5), the values of degradation efficiency after 60 min of Fenton-like rose from 64.5% to 82.0% when hydrogen peroxide was increased from 15.0 to 30.0 mmol/L, respectively. Higher concentrations of H<sub>2</sub>O<sub>2</sub> (37.5 mmol/L) do not significantly enhance removal efficiency; this behavior may be explained by the recombination of hydroxyl radicals with H<sub>2</sub>O<sub>2</sub>, which will result in the scavenging of •OH radicals [12].

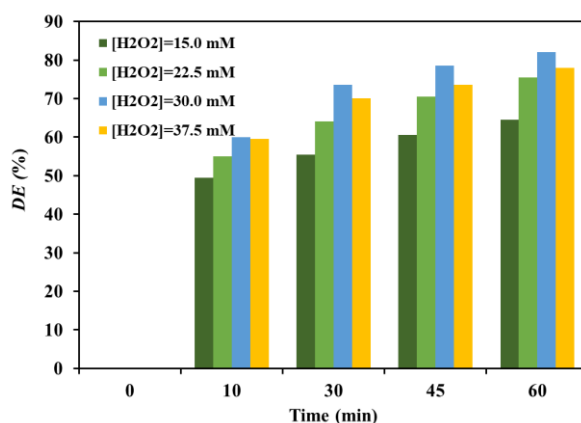


**Fig. (5): Effect of H<sub>2</sub>O<sub>2</sub> concentration**



### 3.4. Effect of pH media

As shown in Figure (6), the pH values of 3, 5, and 7 were investigated. It was discovered that the breakdown of oily wastewater was substantially better at pH 3 than at any other pH. The decrease in the effectiveness of the reaction happened gradually as the pH rose above 3. For instance, when the pH rose from 3 to 7 correspondingly, the removal reduced from 82% to 40.0% after 60 min of the Fenton-like reaction. The instability of  $H_2O_2$  and the limited oxidation capacity of the hydroxyl radical in this environment can be used to explain why the breakdown of oily wastewater is reduced at pH levels greater than 3 [15]. Accordingly, pH 3 is the optimum for oil degradation when using the green catalyst G-Fe/Pd NPs in a heterogeneous Fenton-like catalytic system.

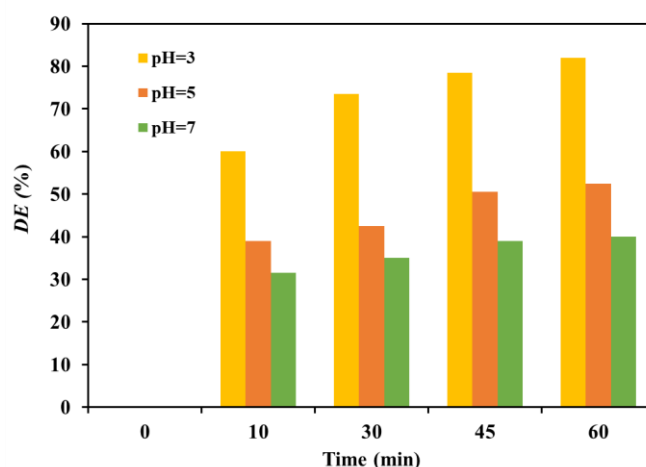
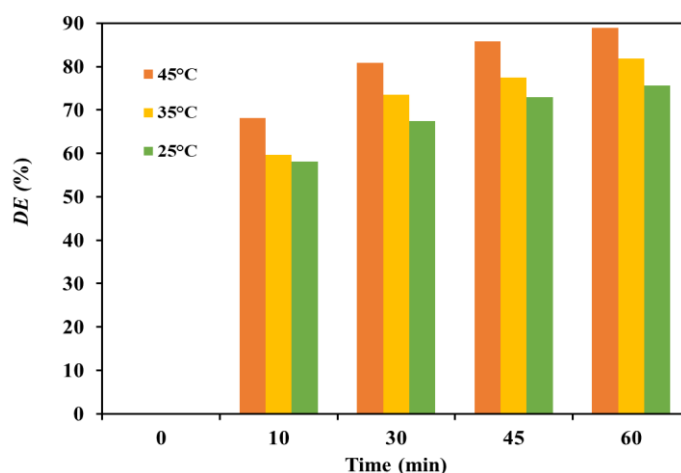


Fig. (6): Effect of pH media on the degradation of oily synthetic wastewater

### 3.5. Effect of temperature

To remove oily wastewater, the effects of several temperatures (25, 35, and 45 °C) on green catalyst G-Fe/Pd NPs (0.375 g/L) and  $H_2O_2$  (30.0 mmol/L) at pH 3 were also investigated. Figure (7) demonstrates how the degrading efficiency grew sharply as the temperature rose. Oil degraded efficiently in 60 minutes at 45 °C, 35 °C, and 25 °C, respectively, at rates of 88.9%, 81.8%, and 75.6%. The mobility of oil pollutants from the solution to the surface of the green catalyst G-Fe/Pd NPs was enhanced when the temperature was raised, which may explain why the Fenton-like reaction was largely reliant on temperature [10].



**Fig. (7): Effect of temperature on the degradation efficiency of oily wastewater**

### 3.6. Kinetics and thermodynamic studies

The linear versions of the first-order, second-order, and Behnajady-Modirshahla-Ghanbary (BMG) kinetic models, as indicated in Equations. (2) to (4), were each used to determine the degradation rate [8].

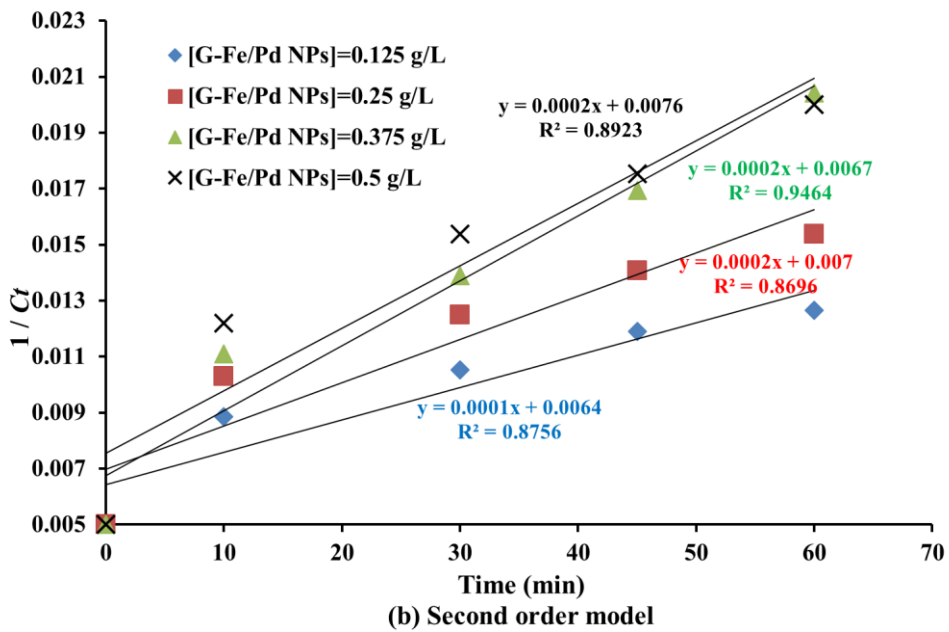
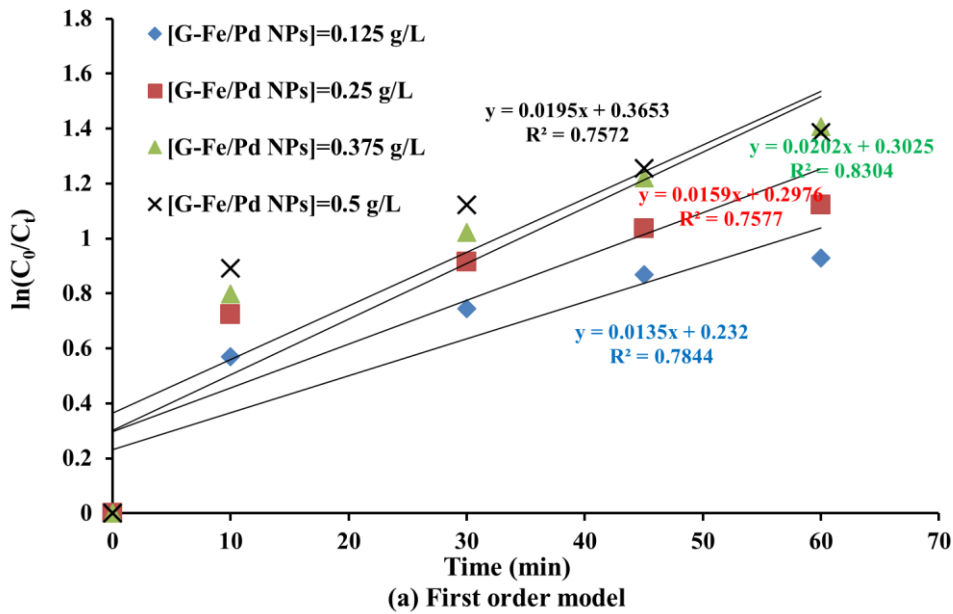
$$\ln \frac{C_0}{C_t} = k_1 \cdot t \quad \text{First-order} \quad (2)$$

$$\frac{1}{C_t} - \frac{1}{C_0} = k_2 \cdot t \quad \text{Second-order} \quad (3)$$

$$\frac{t}{[1 - (C_t/C_0)]} = m + b \cdot t \quad \text{BMG} \quad (4)$$

where  $k_1$  and  $k_2$  are the kinetic rate constants of first and second-order kinetic models, respectively,  $C_0$  and  $C_t$  are the concentration of COD ( $\text{mgO}_2/\text{L}$ ) for the oily wastewater, at the initial and given time  $t$  (min). While  $m$  and  $b$  are two constants concerning initial reaction rate and maximum oxidation capacity, respectively.

At various concentrations of G-Fe/Pd NPs, Figure 8 displayed the linear plots of the kinetics data for the first-order, second-order, and BMG models. Because the correlation coefficient values of the BMG model are often greater than those of the First and Second-order Kinetic models, all data are extremely well fit by this model. These findings agree with previous studies [8], [14].



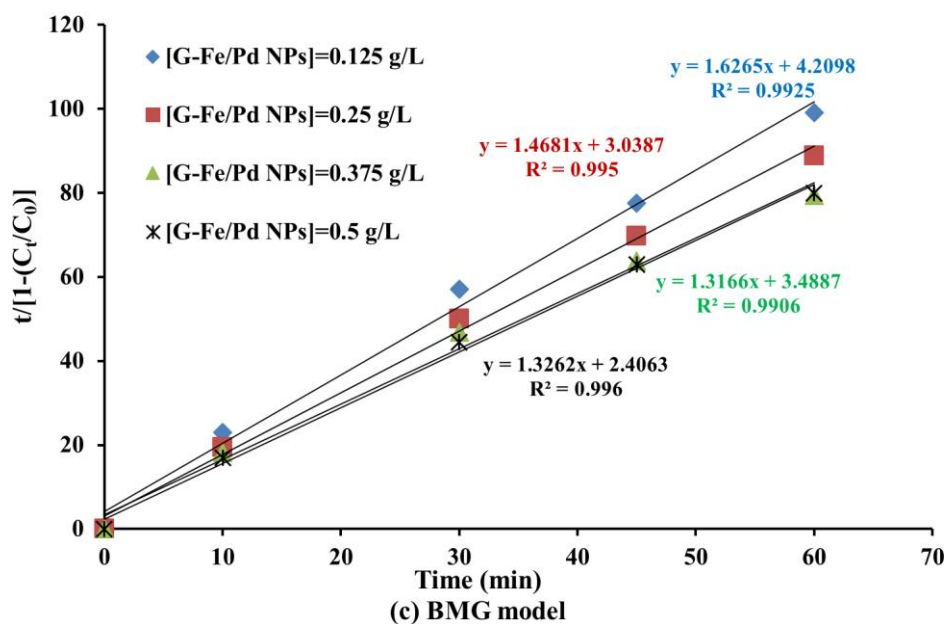


**Fig. (8):** Linear plots of kinetics data of the first-order, second-order, and BMG models at various concentrations of G-Fe/Pd NPs.

The following equations are used for calculating the standard Gibbs free energy change ( $\Delta G^0$ ), enthalpy change ( $\Delta H^0$ ), and entropy change ( $\Delta S^0$ ) for the heterogeneous Fenton reaction [18]:

$$K_d = (C_0 - C_e) / C_e \times (V/m) \quad (5)$$

$$\Delta G^0 = -RT \ln K_d = \Delta H^0 - T\Delta S^0 \quad (6)$$

$$\ln K_d = (\Delta S^0 / R) - (\Delta H^0 / RT) \quad (7)$$

where  $C_e$ ,  $V$ , and  $m$  are the COD of oily wastewater at equilibrium, the volume of oily solution in a liter, and the amount of G-Fe/Pd NPs in grams, respectively. These values can be found in Equation (5). where  $T$  is the temperature of the Fenton-like reaction in Kelvin,  $R$  is the universal gas constant (8.314 J/mol.K), and  $K_d$  is the equilibrium constant (L/g). Equation (6) can be used to get the values of  $\Delta G^0$ , whereas Figure (9) plot of  $\ln K_d$  vs  $1/T$  can be used to determine the values of  $\Delta H^0$  and  $\Delta S^0$ .

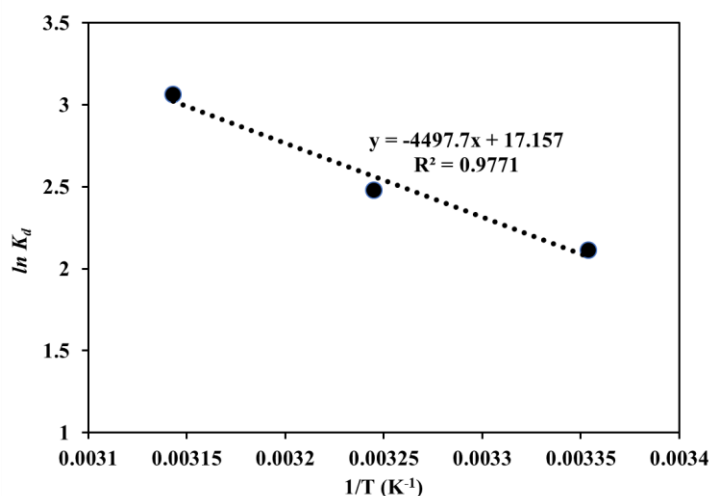


**Fig. (9): Relationship between  $\ln K_d$  against  $1/T$  for thermodynamic constants**

The results from Table (2) demonstrate that the Fenton-like reaction is spontaneous and endothermic, respectively, as demonstrated by the negative values of  $\Delta G^0$  and the positive values of  $\Delta H^0$ . According to Table (2), the reaction's temperature increased the degree of spontaneity in the Fenton-like reaction. The Fenton-like reaction of oil over green catalyst G-Fe/Pd NPs results in an increase in randomness at the solid/solution interface, according to the positive value of  $\Delta S^0$ . This result is in agreement with a previous study for the removal of malachite green dye using a Fenton-like ( $\text{Fe}^{3+}/\text{H}_2\text{O}_2$ ) reaction at a range of temperatures, from 25 to 55 °C [21]. The findings showed the spontaneous and endothermic nature of the malachite green dye's Fenton-like process.

**Table (4) Thermodynamic functions  $\Delta G^0$ ,  $\Delta H^0$ , and  $\Delta S^0$**

Temperature (K)	$\ln K_d$ (L/g)	$\Delta G^0$ (kJ/mol)	$\Delta H^0$ (kJ/mol)	$\Delta S^0$ (kJ/mol K)
298.15	2.112	-5.236	37.393	0.142
308.15	2.478	-6.348		
318.15	3.063	-8.103		

#### **4. Conclusions**

In this study, iron/palladium bimetallic nanoparticles (G-Fe/Pd NPs) were produced using an aqueous extract of eucalyptus plant leaves and utilized to remove synthetic oily wastewater. Zeta potential is used for evaluating the product's stability while FTIR, BET, and particle size are used to describe the green catalyst G-Fe/Pd NPs. The surface area of the G-Fe/Pd NPs was 5.106 m<sup>2</sup>/g, and the average particle size was 182 nm. The effect of process variables on the degrading efficiency was investigated, including the pH of the medium, temperature, and the concentrations of G-Fe/Pd NPs, and H<sub>2</sub>O<sub>2</sub>. After 60 minutes of a Fenton-like reaction, the removal efficiency was 88.9% under the experimental circumstances of 0.375 g/L of G-Fe/Pd NPs, 30.0 mmol/L of H<sub>2</sub>O<sub>2</sub>, temperature 45°C, and a pH of 3.0. All Fenton-like reaction parameter systems appeared to fit the BMG model better, according to the kinetic analyses. The Fenton-like reaction is extremely endothermic and spontaneous, according to research done on the thermodynamic characteristics of the Fenton-like system.

#### **Acknowledgments**

The authors express their profound gratitude to the Environment, Water and Renewable Energy Directorate/ Ministry of Science and Technology in Iraq for providing all the required facilities and support.

## References:

- [1] M. Ismail, K. Akhtar, M. I. Khan, T. Kamal, M. A. Khan, A. M. Asiri, J. Seo, and S. B. Khan, “Pollution, toxicity and carcinogenicity of organic dyes and their catalytic bio-remediation”, *Current Pharmaceutical Design*, vol. 25, no. 34, pp. 3645–3663, 2019. <https://doi.org/10.2174/1381612825666191021142026>
- [2] S. Jafarinejad and S. C. Jiang, “Current Technologies and future directions for treating petroleum refineries and Petrochemical Plants (PRPP) wastewaters”, *Journal of Environmental Chemical Engineering*, vol. 7, no. 5, p. 103326, 2019. <https://doi.org/10.1016/j.jece.2019.103326>
- [3] F. Xiao, J. Yin, D. Shen, T. Chen, and L. Lv, “Treatment of wastewater from thermal desorption for remediation of oil-contaminated soil by the combination of multiple processes”, *Journal of Chemistry*, vol. 2022, pp. 1–13, 2022. <https://doi.org/10.1155/2022/3616050>
- [4] W. F. Elmobarak, B. H. Hameed, F. Almomani, and A. Z. Abdullah, “A review on the treatment of petroleum refinery wastewater using advanced oxidation processes”, *Catalysts*, vol. 11, no. 7, p. 782, 2021. <https://doi.org/10.3390/catal11070782>
- [5] L. Yu, M. Han, and F. He, “A review of treating oily wastewater”, *Arabian Journal of Chemistry*, vol. 10, pp. S1913-S1922, 2017. <https://doi.org/10.1016/j.arabjc.2013.07.020>
- [6] W. Raza, J. Lee, N. Raza, Y. Luo, K. H. Kim, and J. Yang, “Removal of phenolic compounds from industrial waste water based on membrane-based technologies”, *Journal of Industrial and Engineering Chemistry*, vol. 71, pp. 1–18, 2019. <https://doi.org/10.1016/j.jiec.2018.11.024>
- [7] H. M. Ibrahim and R. H. salman, “Study the optimization of petroleum refinery wastewater treatment by successive electrocoagulation and electro-oxidation systems”, *Iraqi Journal of Chemical and Petroleum Engineering*, vol. 23, no. 1, pp. 31–41, 2022. <https://doi.org/10.31699/ijcpe.2022.1.5>
- [8] A. K. Hassan, M. M. Rahman, G. Chattopadhyay, and R. Naidu, “Kinetic of the degradation of sulfanilic acid Azochromotrop (SPADNS) by Fenton process coupled with ultrasonic irradiation or L-cysteine acceleration”, *Environmental Technology & Innovation*, vol. 15, p. 100380, 2019. <https://doi.org/10.1016/j.eti.2019.100380>

- [9] P. C. Silva, N. P. Ferraz, E. A. Perpetuo, and Y. J. Asencios, “Oil produced water treatment using advanced oxidative processes: Heterogeneous-photocatalysis and photo-fenton”, *Journal of Sedimentary Environments*, vol. 4, no. 1, pp. 99–107, 2019. <https://doi.org/10.12957/jse.2019.40991>
- [10] Y. Liu, B. Zhao, G. Ma, S. Zhang, H. Zhang, and Z. Zhu, “Fenton-like remediation for industrial oily wastewater using Fe<sub>78</sub>SI<sub>9</sub>B<sub>13</sub> metallic glasses”, *Catalysts*, vol. 12, no. 9, p. 1038, 2022. <https://doi.org/10.3390/catal12091038>
- [11] A. Singh, P. K. Gautam, A. Verma, V. Singh, P. M. Shivapriya, S. Shivalkar, A. K. Sahoo, and S. K. Samanta, “Green synthesis of metallic nanoparticles as effective alternatives to treat antibiotics resistant bacterial infections: A Review”, *Biotechnology Reports*, vol. 25, 2020. <https://doi.org/10.1016/j.btre.2020.e00427>
- [12] A. K. Hassan, G. Y. Al-Kindi, and D. Ghanim, “Green synthesis of bentonite-supported iron nanoparticles as a heterogeneous Fenton-like catalyst: Kinetics of decolorization of reactive Blue 238 dye”, *Water Science and Engineering*, vol. 13, no. 4, pp. 286–298, 2020. <https://doi.org/10.1016/j.wse.2020.12.001>
- [13] A. K. Hassan, M. A. Atiya, and I. M. Luaibi, “A green synthesis of iron/copper nanoparticles as a catalytic of Fenton-like reactions for removal of Orange G Dye,” *Baghdad Science Journal*, vol. 19, no. 6, p. 1249, 2022. <https://doi.org/10.21123/bsj.2022.6508>
- [14] M. M. Abdul Hassan, S. S. Hassan, and A. K. Hassan, “Comparative of green-synthesis of bimetallic nanoparticles iron/nickel (Fe/Ni) and supported on zeolite 5A: Heterogeneous Fenton-like for dye removal from aqueous solutions”, *Asian Journal of Water, Environment and Pollution*, vol. 19, no. 5, pp. 53–66, 2022. <https://doi.org/10.3233/ajw220071>
- [15] A. K. Hassan, M. M. Abdul Hassan, and A. F. Hasan, “Treatment of Iraqi petroleum refinery wastewater by advanced oxidation processes”, *Journal of Physics: Conference Series*, vol. 1660, no. 1, p. 012071, 2020. <https://doi.org/10.1088/1742-6596/1660/1/012071>
- [16] M. A. Tony, P. J. Purcell, Y. Q. Zhao, A. M. Tayeb, and M. F. El-Sherbiny, “Photo-catalytic degradation of an oil-water emulsion using the photo-fenton treatment process: Effects and statistical optimization”, *Journal of Environmental Science and Health, Part A*, vol. 44, no. 2, pp. 179–187, 2009. <https://doi.org/10.1080/10934520802539830>



- [17] G. Gopal, K. V. G. Ravikumar, M. Salma, N. Chandrasekaran, and A. Mukherjee, “Green synthesized Fe/Pd and in-situ Bentonite-Fe/Pd composite for efficient tetracycline removal”, *Journal of Environmental Chemical Engineering*, vol. 8, no. 5, p. 104126, 2020. <https://doi.org/10.1016/j.jece.2020.104126>
- [18] M. A. Atiya, A. K. Hassan, and Z. A. Mahmoud, “Fenton-like degradation of direct blue dye using green synthesised Fe/Cu bimetallic nanoparticles”, *Journal of Environmental Engineering and Science*, vol. 18, no. 1, pp. 43–58, 2023. <https://doi.org/10.1680/jenes.22.00025>
- [19] Z. A. Mahmoud, M. A. Atiya, and A. K. Hassan, “Application of UV-A light operating photoreactor for green degradation of direct blue 15 through the photo-fenton-like process: Effects and Box-Behnken optimization”, *Egyptian Journal of Chemistry*, vol. 66, no. 11, pp. 77-91, 2023. <https://doi.org/10.21608/ejchem.2022.149569.6463>
- [20] F. Luo, D. Yang, Z. Chen, M. Megharaj, and R. Naidu, “One-step green synthesis of bimetallic Fe/Pd nanoparticles used to degrade Orange II”, *Journal of Hazardous Materials*, vol. 303, pp. 145–153, 2016. <https://doi.org/10.1016/j.jhazmat.2015.10.034>
- [21] S. Hashemian, “Fenton-like oxidation of malachite green solutions: Kinetic and thermodynamic study”, *Journal of Chemistry*, vol. 2013, pp. 1–7, 2013. <https://doi.org/10.1155/2013/809318>